Inform : Jurnal Ilmiah Bidang Teknologi Informasi dan Komunikasi
Vol.10 No.2 July 2025, P-ISSN : 2502-3470, E-ISSN : 2581-0367

Enhancing Facial Image Restoration Using CNN for Blur Severity Classification and U-Net for Deblurring

Muhammad Hidayat Mauluddin[1], Julian Supardi[2]

[1,2]*Computer Science Department, Universitas Sriwijaya, Indonesia*

[1]mauludindayat@gmail.com

[2]julian@unsri.ac.id (*)

Received: 2025-01-02; Accepted: 2025-03-24; Published: 2025-07-04

Abstract— Blurring facial images can significantly degrade the performance of face recognition and video surveillance applications. Therefore, an effective image restoration method is essential to address this issue. However, existing methods struggle with varying levels of blur severity, limiting their effectiveness. This study proposes a facial image restoration approach that integrates blur severity classification using a Convolutional Neural Network (CNN) with a U-Net-based deblurring model to overcome these challenges. This method ensures that each blurred image is processed using the most suiTable deblurring model, optimizing the restoration process. The dataset used in this study is Flickr-Faces-HQ (FFHQ), to which a Gaussian blur is applied and categorized into five levels: very low, low, medium, high, and very high. They employ the Peak Signal-to-Noise Ratio (PSNR) and the Structural Similarity Index Measure (SSIM) as quantitative metrics to evaluate the model's performance. Experimental results show that the proposed method consistently outperforms fixed kernel size and multi-kernel size deblurring approaches across all blur severities. Specifically, our method achieves a PSNR of 40.001 dB for very low blur severity and an SSIM of 0.990. For low severity, it attains a PSNR of 31.104 dB and an SSIM of 0.946. For medium severity, the results are 27.995 dB (PSNR) and 0.874 (SSIM). At high severity, our model achieves a PSNR of 28.896 dB and an SSIM of 0.855. Finally, for very high severity, the PSNR drops to 26.566 dB, with an SSIM of 0.812. These results demonstrate the effectiveness of the proposed method in enhancing image clarity across different blur levels while preserving facial details. This research contributes to the development of more adaptive and efficient image restoration techniques, particularly for applications that require high-quality facial images, such as face recognition and video surveillance.

Keywords— Blur Severity Classification; Image Deblurring; Convolutional Neural Network; CNN; U-Net.

I. INTRODUCTION

Facial images are crucial in various applications, including facial recognition and video surveillance. However, facial images often experience several problems. One of them is blurry. Blur reduces image clarity. Blur in the image can be caused by several factors, such as an out-of-focus lens, camera movement, and object movement [1][2]. Blur in facial images can affect the accuracy of applications such as facial recognition in identifying faces. Therefore, deblurring facial images is a critical topic in computer vision research, aiming to improve the performance of facial recognition systems in identifying faces, as seen in research [3]. Several studies have been conducted to develop methods for improving the quality of blurred images. The focus of existing research varies, ranging from the development of the architecture used and the framework to handling specific blur problems, such as how to perform image deblurring with a wide range of severity, which is explained in research [4][5].

The study "Enhancing Facial Image Clarity: Deblurring Gaussian Blur with UNET++ Architecture" focused on deblurring facial images affected by Gaussian blur using the UNET++ architecture. This study successfully developed an image deblurring model with a Structural Similarity Index Measure (SSIM) value of 0.983 for a kernel size of 3 × 3. However, the SSIM results from this study are relatively high. This study focuses on specific severities of blur. specifically, they only handle blur with kernel sizes of 3 x 3, 5 x 5, and 7 x 7 using different models [6]. This approach limits the model's ability to handle images with more varied levels of blur, especially those with a different kernel size from the image on which the model was trained, thus preventing the model from being optimized to handle a wider range of blur levels.

Another study titled "Blind Face Image Deblurring with Enhancement" developed a model to handle blurred images with various kernel sizes between 13x13 and 27x27 using the Generative Adversarial Network (GAN) architecture [7]. Although this study successfully covered several severities, the results were relatively suboptimal. This is due to the use of a single model designed to handle various levels of blurring severity. This approach reduces the model's ability to restore images at a certain level of blurring severity effectively. Similar approaches have been observed in other studies, such as those in [1][8][9]. Despite using a model capable of handling various levels of blurring, the results are often suboptimal due to the difficulty in adapting to various levels of severity. In other words, applying a single model to handle various levels of blurring prevents it from focusing on restoring images with a certain level of severity, which ultimately reduces the quality of recovery under certain blurring conditions.

To address these challenges, this study proposes a novel approach for optimizing the restoration of blurred facial images, particularly those affected by Gaussian blur. Previous studies often suffer from significant limitations: some only focus on handling a narrow range of blur severities, such as kernel sizes between 3x3 and 7x7, which restricts their applicability to real-world scenarios with more varied blur levels [6]. Others attempt to manage various blur severities using a single deblurring

DOI : https://doi.org/10.25139/inform.v10i2.9542

model. Still, this approach often yields suboptimal results due to the lack of specialization for different blur levels [1][7]–[9]. These shortcomings limit the effectiveness of existing methods in restoring images across a range of blur severities.

The proposed method integrates a Convolutional Neural Network (CNN) for blur severity classification with a U-Net-based deblurring model tailored for each specific blur severity level. This approach enables more precise and effective restoration by processing each image using a specialised deblurring model tailored to its identified level of blur severity. Furthermore, it enhances the efficiency and accuracy of the deblurring process compared to previous methods. This study applies the deblurring process to the entire image, not just the facial region. This ensures a more comprehensive restoration, improving the overall image quality rather than focusing solely on the face. This approach can be likened to an office with specialized teams, where each team focuses on a particular task, resulting in greater efficiency and effectiveness. Similarly, this study's approach ensures that images with varying degrees of blur are restored with greater focus and accuracy, ultimately overcoming the limitations of prior research.

II. Research Methodology

This study has four key stages to achieve the research objectives of optimizing the restoration of blurry facial images. Fig. 1 provides a detailed explanation of the stages conducted in this study.

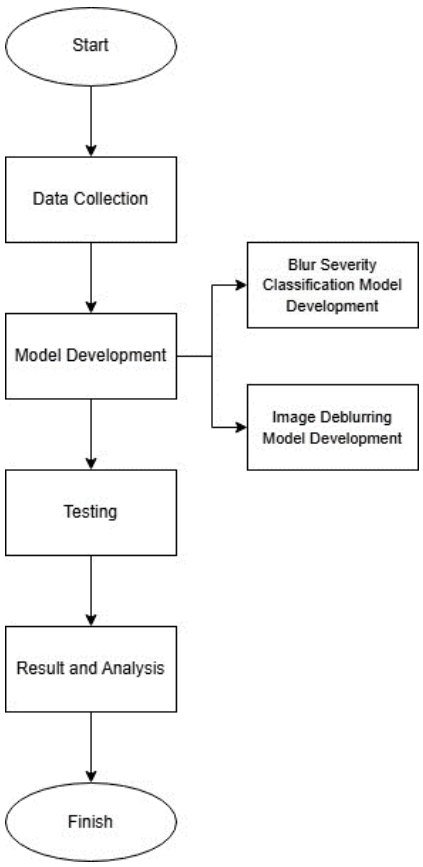

Fig. 1 Research Stages

Fig.1 illustrates the research stages: data collection, model development, blurred level classification, image deblurring model development, testing, and result analysis. Each stage plays a crucial role in achieving the research objective of optimizing the restoration of blurry facial images.

A. Proposed Method

The proposed method in this study is an approach that separates the image deblurring model based on five levels of severity, which are then integrated with the blur severity classification model. The integration aims to ensure that the selected deblurring model is the most suitable table model for overcoming the blur in the image. The approach proposed in Fig.2 is based on this research.

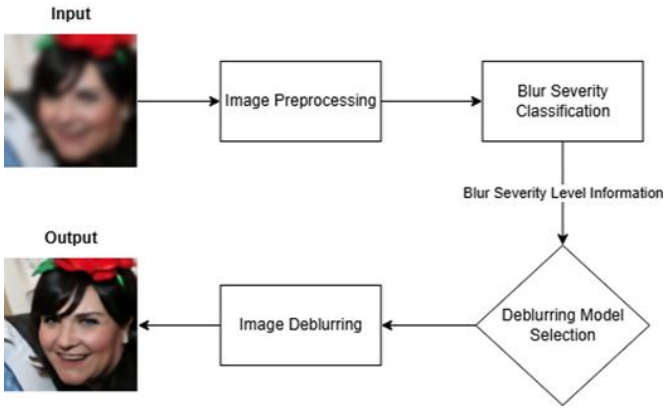

Fig.2 Proposed Approach

This method aims to overcome the limitations of conventional approaches by providing more accurate and optimal image restoration at various levels of blur severity.

a) Input: The blurred facial image to be deblurred will serve as the input.

b) Image pre-processing: The input image is then normalized to the range of 0 to 1, as required by the model.

c) Blur Severity Classification: The image will be processed through a classification system to determine the severity of the blur.

d) Deblurring Model Selection: Information from the blurring level classification process will be used to select the most appropriate deblurring model based on the identified severity category.

e) Image Deblurring: In this stage, the selected deblurring model is used to process the blurred image.

f) Output: These processes will restore the image.

B. Data Collection

The dataset used in this study consists of facial images obtained and accessible through the GitHub repository, specifically the Flickr-Faces-HQ Dataset (FFHQ). This dataset was chosen because it is fairly well-known and provides various facial attributes, including age differences, skin colour,

DOI : https://doi.org/10.25139/inform.v10i2.9542

glasses, and other features. The diversity in the FFHQ dataset ensures that the model is exposed to a wide range of facial features and characteristics, thereby enhancing the generalization of the developed system. The images used in this study are 128x128 in size and are available on FFHQ [4][10]. A few sample images from this dataset are shown in Fig.3.

Fig.3 FFHQ Dataset

This study applies a Gaussian blur to the entire image, including the face and background. This ensures that the model learns to restore the entire image rather than focusing solely on the facial area, making it more applicable to real-world scenarios. Table I details that the dataset is processed by adding a Gaussian blur effect with various kernel sizes.

TABLE I
KERNEL SIZE PARAMETERS FOR DIFFERENT BLUR SEVERITIES

Blur Severity	Kernel Size (Parameters)
Very Low	3x3, 5x5, 7x7
Low	9x9, 11x11, 13x13
Medium	15x15, 17x17, 19x19
High	21x21, 23x23, 25x25
Very High	27x27, 29x29, 31x31

Applying the Gaussian blur effect with various kernel sizes aims to produce a dataset representing various levels of blur usually encountered in real-world applications.

Two thousand images were used for training the blur severity classification model, 10000 images were used for training, 20% were set aside for validation, and 12000 images were used for testing. The total number of images used for the model was twelve thousand.

For the image deblurring model, 12000 pairs of images were used for each blur severity level. Each pair consists of *X* (a blurred image) and Y (a clean image), where *Y* serves as the target during training. Ten thousand pairs were used for training, with 20% (2000 pairs) allocated for validation. Two thousand pairs were reserved for testing. This large dataset ensured the effectiveness of both models in classifying blur severity and restoring images.

C. Model Development

a) Blur Severity Classification: A blur-level classification model was developed using Convolutional Neural Networks (CNN), which is effective in classifying image blur with relatively high accuracy [11]–[13]. With this architecture, the model is expected to accurately distinguish between image blur levels.

b) Image Deblurring Model Development: U-Net is the model architecture used for image deblurring. U-Net was chosen because of its proven success in image restoration tasks [6][14][15]. This model architecture handles different blur levels, ensuring each severity level has a dedicated deblurring model to restore image clarity.

D. Testing

At this stage, testing will be conducted on the model that has been built and on the system after integration between the classification model and image deblurring.

a) Testing the Blur Severity Classification Model: The blur severity classification model will be tested using a dataset that was never used in training. The evaluation is performed using standard classification metrics, where Equations (1), (2), (3), and (4) are used to calculate accuracy, precision, recall, and F1-score, respectively. These metrics are commonly used in classification tasks [16].

$$Accuracy = \frac{Number\ of\ correct\ predictions}{Total\ number\ of\ data} \quad (1)$$

$$Precision = \frac{True\ Positives}{True\ Positives + False\ Positives} \quad (2)$$

$$Recall = \frac{True\ Positives}{True\ Positives + False\ Negatives} \quad (3)$$

$$F1 - Score = 2 \times \frac{Precision \times Recall}{Precision + Recall} \quad (4)$$

Testing the Image Deblurring Models: The developed image deblurring model will be tested for effectiveness using a previously unused blur dataset. The deblurring model is evaluated using two commonly used image quality metrics: PSNR (Peak Signal-to-Noise Ratio) and SSIM (Structural Similarity Index Measure), as shown in Equations (5) and (6), respectively. These metrics are widely used in image restoration tasks, such as deblurring, because they provide complementary perspectives. PSNR measures pixel-level fidelity, while SSIM assesses perceptual quality and structural similarity [17][18]. The PSNR is calculated using Equation (5), where MAX represents the maximum possible pixel value, and MSE represents the Mean Squared Error between the original and deblurred images.

$$PSNR = 10 \cdot \log_{10}\left(\frac{MAX^2}{MSE}\right) \quad (5)$$

Structural Similarity Index Measure (SSIM) using Equation (6). SSIM evaluates structural, pattern, and texture similarity between the original and deblurred images, with values ranging from 0 to 1 [17][18].

$$SSIM(x,y) = \frac{(2\times\mu_x\times\mu_y\times C_1)(2\times\sigma_{xy}+C_2)}{(\mu_x^2+\mu_y^2+C_1)\ (\sigma_x^2+\sigma_y^2+C_2)} \quad (6)$$

DOI : https://doi.org/10.25139/inform.v10i2.9542

b) Integrated System Testing: After the developed models are tested individually, they are integrated and tested as a whole system. This test evaluates the effectiveness of the integrated system in restoring blurred images.

E. Result Analysis

The results obtained will then be analyzed to evaluate the effectiveness of the proposed method in restoring blurred facial images in comparison to methods from previous studies. This stage provides valuable insights into the advantages and disadvantages of the proposed method, which serves as a basis for drawing conclusions and offering recommendations for future research.

III. Result and Discussion

The results of the study should be written clearly and concisely. The discussion should describe the significance of the research results, rather than merely repeating them. Avoid using citations and excessive discussion of published literature.

A. Data and Data Collection

The dataset obtained from FFHQ is then synthetically processed with a blur effect by applying a Gaussian blur from OpenCV. The kernel size parameters used follow the provisions in Table I, where the dataset will be grouped into five categories: very low, low, medium, high, and very high. This aims to ensure clear visual differences for each category of blur severity [19]. Fig. 4 shows examples illustrating the visual differences between the original and blurred images, as well as the visual differences for each level of blur severity.

(a) (b)

Fig.4 Original Image (a) and Blurred Image (b)

As shown in Fig.4, the comparison between the original image (a) and the blurred image (b) illustrates the differences in blur intensity across various levels of severity. This aligns with the research objective of classifying blur severity and restoring images affected by varying blur levels.

B. Model Development

1) Blur Severity Classification

The blur level classification model is developed using a Convolutional Neural Network (CNN). The CNN architecture used at this stage is a modification of the architecture in the study [11], which uses Simplified-Fast-Alexnet (SFA) to develop a blur classification model. This architecture has been proven effective in performing blur classification. A visual representation of the CNN architecture implemented in this study is shown in Fig.5.

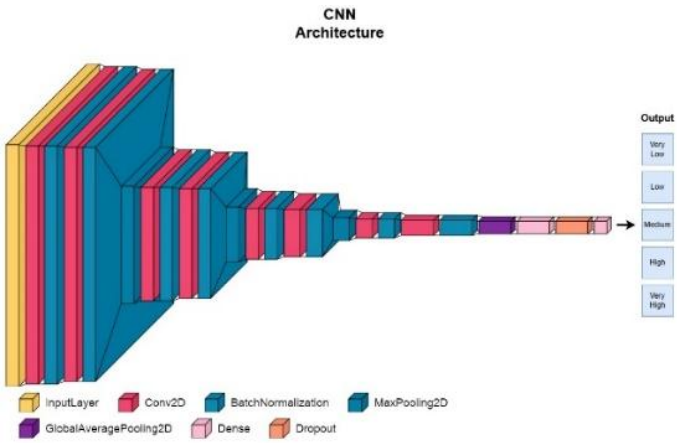

Fig.5 CNN Architecture for Blur Severity Classification

The CNN architecture used in this study comprises the following types of layers.

a) Input Layer: During training, the model receives images with dimensions (128 x 128 x 3). Flexible input sizes (None, None, 3) enable the model to process images of various sizes without requiring modifications to the architecture.

b) Convolution and Pooling (Feature Extraction): The model consists of four blocks, each consisting of a Conv2D layer with a 3x3 kernel and a ReLU activation function. Each convolutional layer is followed by a batch normalization layer to normalize the output and ends with a MaxPooling2D layer with a pool size of 2x2. The number of filters in the convolutional layer increases gradually in each block, namely 64, 128, 256, and 512 [20][21].

c) Global Average Pooling: After passing through the convolution and pooling blocks, the GlobalAveragePooling2D layer is applied. This layer aims to reduce the dimensionality of the features without losing important information.

d) Fully Connected Layers: A fully connected layer consisting of a dense layer with 1024 units and a ReLU activation function. Followed by a Dropout layer with a drop rate of 0.5 to reduce the risk of overfitting. Then, enter the final layer, or output layer, which is a Dense layer with five units. The Softmax activation function is applied to this layer to produce probability predictions for each class [21]. The detailed CNN architecture is summarized in Table II.

TABLE II
CNN ARCHITECTURE FOR BLUR SEVERITY CLASSIFICATION

Layer (Type)	Output Shape
Input Layer	(None, 128, 128, 3)
Conv2D + BatchNorm	(None, 126, 126, 32)
Conv2D + BatchNorm	(None, 124, 124, 64)
MaxPooling2D	(None, 62, 62, 64)
Conv2D + BatchNorm	(None, 60, 60, 64)
Conv2D + BatchNorm	(None, 58, 58, 128)

DOI : https://doi.org/10.25139/inform.v10i2.9542

Layer (Type)	Output Shape
MaxPooling2D	(None, 29, 29, 128)
Conv2D + BatchNorm	(None, 27, 27, 128)
Conv2D + BatchNorm	(None, 25, 25, 256)
MaxPooling2D	(None, 12, 12, 256)
Conv2D + BatchNorm	(None, 10, 10, 256)
Conv2D + BatchNorm	(None, 8, 8, 512)
GlobalAveragePooling2D	(None, 512)
Dense	(None, 512)
Dropout	(None, 512)
Output Dense (Softmax)	(None, 5)

The hyperparameter settings used for the training process of the blur severity classification model are listed in Table III. They employed the Grid Search method to tune the optimizer and learning rate, thereby identifying the optimal hyperparameters. This approach systematically evaluated various combinations of these hyperparameters to determine the configuration that achieved the highest validation accuracy. For efficiency, only 10% of the training dataset was used during hyperparameter tuning, which reduced computational time while still providing reliable results. Once the optimal hyperparameters were identified, the final model was trained on the full dataset to maximize performance.

TABLE III
HYPERPARAMETERS FOR BLUR SEVERITY CLASSIFICATION MODEL TRAINING

Hyperparameter	Value
Optimizer	[Adam, RMSprop, SGD]
Loss	Categorical Crossentropy
Epochs	100
Learning rate	[0.01, 0.001, 0.0001]
Batch size	32

This research also implemented callbacks, including ModelCheckpoint and EarlyStopping, with a patience of 25, to ensure optimal performance during training. As summarized in Table IV, a hyperparameter tuning process was conducted using grid search. The results showed that the best configuration was achieved using the Adam optimizer with a learning rate of 0.001, resulting in a validation accuracy of 94%. Adam was chosen for its adaptive learning rate, which consistently outperformed SGD and RMSprop. A learning rate of 0.001 provided the best balance between convergence speed and accuracy, thereby avoiding issues such as overfitting or slow training.

TABLE IV
HYPERPARAMETER TUNING USING GRID SEARCH

Optimizer	Learning Rate	Accuracy Score
Adam	0.01	0.88
Adam	**0.001**	**0.94**
Adam	0.0001	0.918
SGD	0.01	0.932
SGD	0.001	0.874
SGD	0.0001	0.908
RMSprop	0.01	0.918
RMSprop	0.001	0.886
RMSprop	0.0001	0.738

2) Image Deblurring

We use the U-Net architecture to develop the deblurring model, which has been proven effective in performing blurred image restoration [6][22]. The architecture is modified to improve the ability to restore facial images affected by varying degrees of blur. The layer structure of the modified U-Net architecture is illustrated in Fig.6.

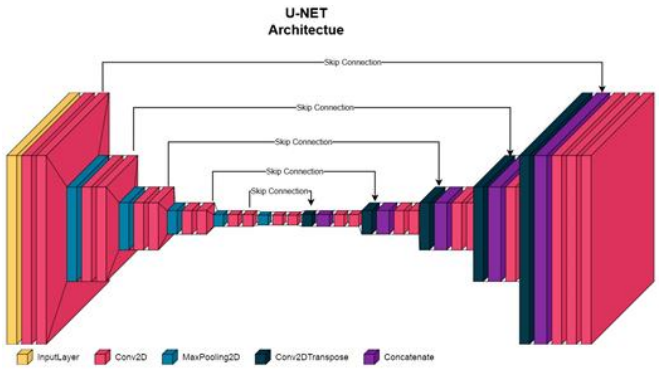

Fig.6 U-Net Architecture for Image Deblurring

The U-Net architecture consists of the following components:

a) Input Layer: The images used in model training are 128x128 pixel images. However, the model can accept input images with flexible dimensions (None, None, 3) for various image sizes.

b) Encoder: As illustrated in Fig.7, the encoder comprises five sequential blocks. Each consists of a conv2D Layer that applies 128 filters with a 3×3 kernel using the ReLU activation function, and a maxPooling2D Layer reduces the spatial dimensions by a factor of two using a pooling size of 2×2. This process progressively extracts features at multiple levels of abstraction while reducing the spatial resolution. Skip connections transfer features from each encoder block to the corresponding decoder block. These skip connections preserve spatial information, which is critical for restoring fine details in the decoding phase.

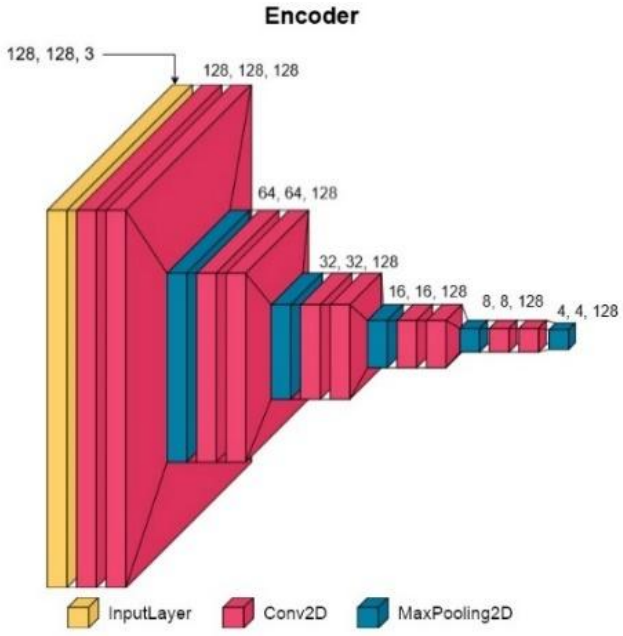

Fig.7 Encoder

DOI : https://doi.org/10.25139/inform.v10i2.9542

c) Bottleneck: As shown in Fig. 8, the bottleneck serves as the transition phase between the encoder and decoder components of the U-Net architecture. It utilizes additional Conv2D layers with 128 filters to extract deeper, more abstract features and capture contextual information. This stage is crucial for identifying global patterns and structures within the image, which are essential in guiding the reconstruction process during the decoding phase.

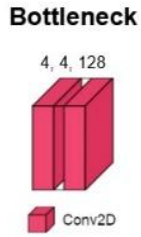

Fig.8 Bottleneck

d) Decoder: As illustrated in Fig.9, the decoder comprises five Conv2DTranspose blocks that progressively upsample the image dimensions to their original resolution. This upsampling restores spatial detail, while skip connections merge the decoder features with corresponding features from the encoder. Combining high-level context with low-level details ensures that structural coherence and fine textures are retained, enabling the model to generate sharp and high-quality restored images.

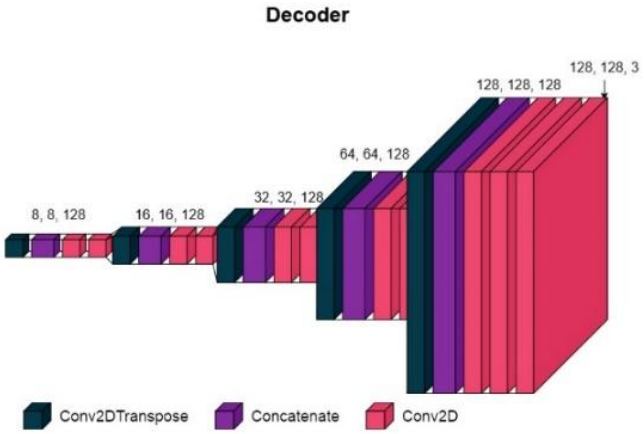

Fig.9 Decoder

e) Output Layer: The output layer consists of a Conv2D layer with a 3x3 kernel and sigmoid activation, generating an image of pixel values ranging from 0 to 1.

The hyperparameters used for training the image deblurring models are summarized in Table V. These include the optimizer, loss function, number of epochs, learning rate options, and batch size.

TABLE V
HYPERPARAMETERS FOR IMAGE DEBLURRING MODEL TRAINING

Hyperparameter	Value
Optimizer	[Adam, RMSprop, SGD]
Loss Function	Mean squared error
Epochs	100
Learning rate	[0.01, 0.001, 0.0001]
Batch size	32

Hyperparameter tuning was conducted on the optimizer and learning rate using the Grid Search method to identify the best configuration. Additionally, callbacks such as ModelCheckpoint and EarlyStopping (with a patience parameter of 10) were implemented to optimize the training process and ensure the model achieved the best performance. For efficiency, only 10% of the training dataset was used during the tuning phase to reduce computational time while providing meaningful results.

TABLE VI
HYPERPARAMETER TUNING

Optimizer	Learning Rate	Loss Score
Adam	0.01	0.253
Adam	**0.001**	**0.0009**
adam	0.0001	0.0011
SGD	0.01	0.006
SGD	0.001	0.053
SGD	0.0001	0.075
RMSprop	0.01	0.246
RMSprop	0.001	0.0015
RMSprop	0.0001	0.0012

The detailed results of the tuning process are presented in Table VI. Among all configurations, the Adam optimizer with a learning rate of 0.001 achieved the lowest loss score of 0.0009, demonstrating superior performance. Adam's adaptive learning rate helped it efficiently minimize the MSE during training. In contrast, SGD and RMSprop yielded higher loss scores, indicating less optimal convergence. A learning rate of 0.01 consistently produced subpar results, likely due to overshooting during gradient updates. These findings highlight the effectiveness of using Adam with a moderate learning rate for training the image deblurring model.

C. Testing

1) Testing of Blur Severity Classification Model

The Blur Severity Classification model was tested with 2000 prepared test images. The model's performance is summarized in Table VII, where the precision, recall, F1-score, and accuracy are displayed for each blur severity level. The model achieved an average accuracy of 95%, with Very High and Very Low severity levels achieving the highest performance. These results indicate that the model effectively classifies blur severity levels.

TABLE VII
PERFORMANCE METRICS OF BLUR SEVERITY CLASSIFICATION MODEL

Severity Level	Precision	Recall	F1-Score	Accuracy
Very low	0.991	0.978	0.984	0.95
Low	0.939	0.988	0.963	0.95
Medium	0.968	0.921	0.944	0.95
High	0.938	0.885	0.911	0.95
Very High	0.918	0.979	0.947	0.95

Fig. 10 displays the confusion matrix to provide a clearer picture of the model's performance in terms of classification. The confusion matrix in Fig. 10 above shows that the model can classify well across all severity categories. However, the

DOI : https://doi.org/10.25139/inform.v10i2.9542

very high and medium categories require special attention to reduce the level of classification errors.

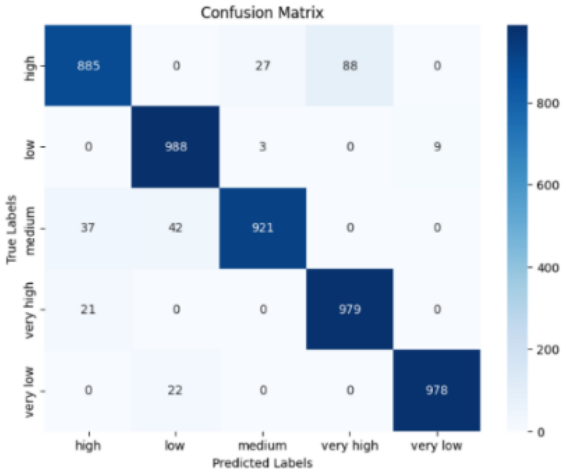

Fig.10 Confusion Matrix for Blur Severity Classification Model

2) Testing of Image Deblurring Model

The performance of the deblurring model is tested using 2000 previously unused images. Table VIII presents the average performance results of the deblurring model at each blur severity level, evaluated using the PSNR (Peak Signal-to-Noise Ratio) and SSIM (Structural Similarity Index Measure) metrics.

The model performs well at lower blur severity levels, with PSNR and SSIM values indicating high-quality restoration. However, as the blur severity increases, the quality of the deblurring results gradually decreases.

TABLE VIII
PERFORMANCE OF DEBLURRING MODEL FOR DIFFERENT BLUR SEVERITIES

Deblurring Model (Blur Severity)	PSNR (dB)	SSIM
Very low	37.362	0.974
Low	31.802	0.926
Medium	28.929	0.870
High	27.268	0.821
Very High	25.807	0.772

3) Integrated System Testing

Integrated system testing was conducted using 5 test images with different levels of blur severity. The integrated system was tested as a whole, considering its classification and image deblurring models. The results of the integrated system testing are presented in Table IX. Overall, the integrated system performs quite well because the classification model can accurately classify the severity of the image's blur, and the image deblurring model can significantly improve the image quality compared to the blurred image before restoration.

TABLE IX
COMPARISON OF BLUR SEVERITY PREDICTION AND DEBLURRING PERFORMANCE

Test Image	Actual Blur Severity	Predicted Blur Severity / Prediction Accuracy	PSNR / SSIM Before Deblurring	PSNR / SSIM After Deblurring	Output
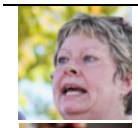	Very Low	Very Low / 100%	31.317 / 0.949	40.001 / 0.990	
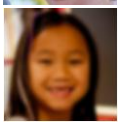	Low	Low / 99.997%	23.662 / 0.766	31.104 / 0.946	
	Medium	Medium / 99.873%	21.834 / 0.645	27.995 / 0.874	
	High	High / 99.847%	20.347 / 0.549	28.896 / 0.855	
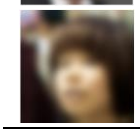	Very High	Very High / 99.472%	18.981 / 0.517	26.566 / 0.812	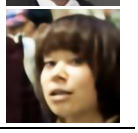

D. Result Analysis

1) Analysis of Blur Severity Classification Model Results

The blur classification model demonstrated strong performance with an average accuracy of 95%. Table VII and the confusion matrix in Fig. 10 show that the very low and very high severity levels yielded higher results than the other categories. This indicates that the model effectively classifies images in extreme blur severity levels.

In contrast, medium and high severity levels showed slightly lower results, indicating that the model faces more challenges distinguishing between these categories. This may be because the visual characteristics of images in medium and high severity levels often look similar, which can result in reduced

DOI : https://doi.org/10.25139/inform.v10i2.9542

classification accuracy in these categories. Therefore, in further research, improvements are expected to be made to the architecture used for blur severity classification to improve the model's accuracy in classifying blur severity levels. The blur severity classification stage is very important in the method proposed in this study. Because if the blurred image enters the wrong deblurring model, the resulting image will not be optimal.

2) Analysis of Image Deblurring Model Results

The results from the image deblurring model test are shown in Table VIII. The model performs relatively well at a low blur severity level, achieving a PSNR value of 37.362 dB and an SSIM of 0.974. This is likely because the image blur intensity at that severity level is still very low, meaning there is no significant difference between the blurry and clean images.

However, as the blur severity increases, the quality of the restored image declines significantly. At the very high blur severity level, the PSNR drops to 25.807 dB, and the SSIM drops to 0.772, indicating the model's reduced ability to recover image details as blur severity increases. This decline is primarily due to the extreme loss of high-frequency details in heavily blurred images. Intense blurring results in the loss of fine-grained texture and structural details, thereby complicating the model's ability to reconstruct the original image accurately. Unlike mild or moderate blurs, where enough spatial information remains for the model to infer missing details, very high severity levels result in extensive information degradation, leading to ambiguity in the restoration process.

Another contributing factor is the increasing difficulty in learning a meaningful mapping between heavily blurred and clean images. As the blur severity increases, the clean target image significantly differs from the input, making it harder for the model to generalize and accurately reconstruct fine details.

3) Comparison Analysis

A comparative analysis is conducted between the proposed method and methods in previous studies. The proposed method integrates blur severity classification with a customized deblurring model for each blur severity level. This approach is compared with the Fixed Kernel Size Deblurring Method, which uses a fixed kernel size of 3x3 for deblurring [6], and the Multi Kernel Size Deblurring Method, which employs kernel sizes ranging from 3x3 to 31x31 [1][7]–[9].

To ensure a fair comparison, the methods from previous studies are rebuilt or replicated to maintain equivalence in other variables, such as model architecture, training settings, and the number of datasets used. This approach ensures the objectivity of the comparison results. The following Table X presents the Quantitative Performance Comparison:

TABLE X
QUANTITATIVE PERFORMANCE COMPARISON

Test Image	Proposed Method		Fixed Kernel Size Deblurring Method		Multi-Kernel Size Deblurring Method	
	PSNR	**SSIM**	**PSNR**	**SSIM**	**PSNR**	**SSIM**
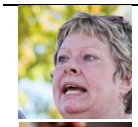	40.001	0.990	**40.527**	**0.991**	35.303	0.978
	**31.104**	**0.946**	24.029	0.778	29.234	0.930
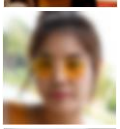	**27.995**	**0.874**	21.952	0.651	27.748	0.865
	**28.896**	**0.855**	21.973	0.650	28.130	0.847
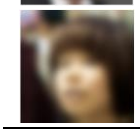	**26.566**	**0.812**	19.876	0.558	25.285	0.780

Based on the comparison results presented in Table X, the proposed method consistently outperforms the comparison methods on all tested images. One key reason for this superior performance is that the proposed method integrates blur severity classification with a customized deblurring model for each severity level. This allows the method to apply the most suiTable deblurring technique based on the identified blur severity, leading to more precise restoration.

The fixed kernel size deblurring method [6] shows good performance on the first test image but experiences a significant decrease in performance on subsequent images. This decrease is due to the model's inability to handle variations in blur that deviate from the fixed kernel size used during training. In other

DOI : https://doi.org/10.25139/inform.v10i2.9542

words, when the blur severity differs from the kernel size, the fixed kernel model struggles to restore the image effectively, leading to poorer results.

On the other hand, the Multi-Kernel Size Deblurring Method [1][7]–[9] attempts to handle various levels of blur severity by using different kernel sizes within a single model. However, this approach suffers from the challenge of generalizing across multiple blur levels within one model. The method does not specialize in any specific severity level, which reduces its ability to restore images optimally. In contrast, the proposed method employs a specific deblurring model tailored to each severity level, thereby ensuring better performance across a wide range of blur variations.

Thus, the proposed method overcomes the limitations of previous methods by targeting blur severity levels directly and applying a model designed for each level. This leads to more accurate restoration, especially for images with higher or more complex blur, ultimately providing superior performance in image quality.

For visual comparison, Table XI displays the images, which demonstrate the proposed method's ability to restore finer details and achieve better clarity, particularly in regions of high blur severity.

TABLE XI
QUALITATIVE VISUAL COMPARISON

Blur Image (Severity Level)	**Ground Truth**	**Proposed Method**	**Fixed Kernel Size Deblurring Method [6]**	**Multi Kernel Size Deblurring Method** [1][7]–[9]
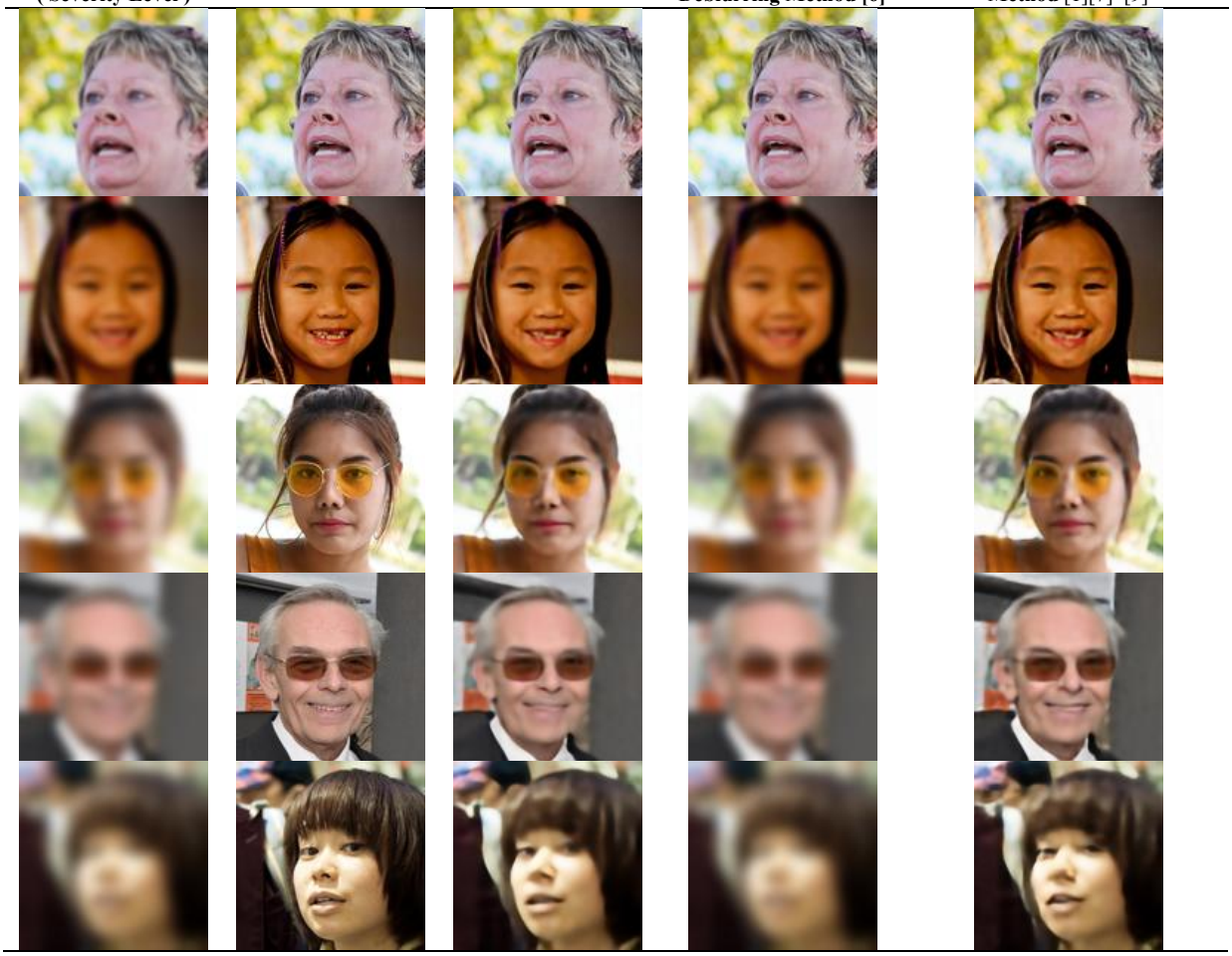				

The results shown in Table XI are consistent with the analysis given in Table IX, where the proposed method consistently outperforms the Fixed Kernel Size and Multi Kernel Size Deblurring methods across all tested images. Although visually, there is no significant difference between the images generated by the proposed method and the Multi Kernel Size Deblurring method. The difference may be very noticeable in broader problem cases.

4) Real-World Testing

To evaluate the practical effectiveness of the proposed method, we tested it on real-world blurry images. Unlike the synthetically blurred dataset, these images exhibit natural blur caused by various factors such as motion, defocus, and mixed blur types. This evaluation helps determine how well the model generalizes beyond controlled training conditions.

DOI : https://doi.org/10.25139/inform.v10i2.9542

Three blurry images from the Labelled Faces in the Wild (LFW) dataset and Google Images were selected and processed using the blur severity classification and deblurring models. The results are summarized in Table XII.

TABLE XII
REAL-WORLD TESTING

Test Image	Predicted Blur Severity / Prediction Accuracy	Output
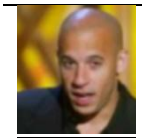	Low / 99.94%	
	Very Low / 99.23%	
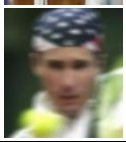	Low / 96.04%	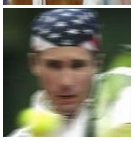

The classification model demonstrated strong performance in predicting blur severity, confirming its reliability even on real-world images. However, the deblurring results varied across different cases. The first image, classified as low blur severity with 99.94% accuracy, was successfully restored, significantly improving clarity and facial details. The second image, classified as very low blur severity with 99.23% accuracy, showed no improvement after deblurring. While the blur was minimal, the motion in the image made it difficult for the model to enhance quality, resulting in little to no visible change. The third image, classified as having low blur severity with 96.04% accuracy, underwent partial restoration but remained messy, with residual blur and artifacts. The natural motion blur from a tennis player was slightly reduced, but the motion effect persisted, showing the model's difficulty in handling motion blur.

These results highlight a key limitation: the model was trained only on Gaussian blur, while real-world blur is more complex. Variations such as motion blur and lens defocus were not included in the training data, making it more challenging for the model to generalize. Despite this, the blur severity classification model performed well and achieved high accuracy in classifying natural blur. However, the deblurring model struggled with more complex blurs, particularly motion blur, underscoring the need for further improvements to handle real-world scenarios effectively.

IV. CONCLUSION

This study presents a novel approach for facial image deblurring that effectively addresses the blur problem through an integrated system combining a CNN-based blur severity classification model with a U-Net-based deblurring model. By separating the deblurring process based on the severity of the blur, the proposed method demonstrates clear advantages over conventional techniques, such as fixed-kernel-size and multi-kernel-based deblurring methods. The primary strength of this system lies in its ability to adapt to different levels of blur, resulting in higher-quality restored images across varying levels of blur severity. Additionally, the proposed method consistently outperforms previous research methods in objective and subjective evaluations, demonstrating its effectiveness in handling Gaussian-blurred images.

Despite the promising results, this study has several limitations. One key limitation is the reliance on a dataset with Gaussian blur only, which restricts its ability to generalize to other types of blurs frequently occurring in the real world, such as motion blur, defocus blur, and mixed blur patterns not included in the training dataset. As a result, the model does not yet perform effectively on real-world blurry images, where the blur characteristics are more complex and diverse. Additionally, while the proposed approach performs well on the FFHQ dataset, its robustness on diverse or real-world datasets containing more complex or mixed blur patterns remains untested, representing an area for future work. Furthermore, the approach involves an additional classification step before deblurring, which introduces extra computational time, particularly when dealing with large-scale datasets or real-time applications.

In terms of performance evaluation, the method demonstrated significant improvements in objective metrics, such as the Peak Signal-to-Noise Ratio (PSNR) and the Structural Similarity Index Measure (SSIM), as well as in subjective evaluation, where the restored images showed visually enhanced clarity and structure. However, more extensive subjective evaluations, possibly involving human raters, could provide deeper insights into the perceptual quality of the restored images.

Future research should address these limitations by exploring more diverse datasets, including real-world blurs, and extending the system's capability to handle mixed or dynamic blur scenarios. Additionally, optimizing the computational efficiency of the model will be crucial for its practical deployment in real-time applications.

REFERENCES

[1] Y. Kim, H. Kwon, and H. Ko, "Facial image deblurring network for robust illuminance adaptation and key structure restoration," *Eng. Appl. Artif. Intell.*, vol. 133, no. PA, p. 107959, 2024, doi: 10.1016/j.engappai.2024.107959.

[2] S. H. Jung, T. Bok Lee, and Y. S. Heo, "Deep Feature Prior Guided Face Deblurring," *Proc. - 2022 IEEE/CVF Winter Conf. Appl. Comput. Vision, WACV 2022*, pp. 884–893, 2022, doi: 10.1109/WACV51458.2022.00096.

[3] S. S. Beulah Benslet and P. Parameswari, "Enhancement of Criminal Facial Image Using Multistage Progressive V-Net for Facial Recognition by Pixel Restoration," *ICST Trans. Scalable Inf. Syst.*, vol. 11, no. 3, 2024, doi: 10.4108/eetsis.3980.

[4] B. Wang, F. Xu, and Q. Zheng, "A survey on facial image deblurring," *Comput. Vis. Media*, vol. 10, no. 1, pp. 3–25, 2023, doi: 10.1007/s41095-023-0336-6.

[5] Z. Yu, "Image deblurring: comparison and analysis," *J. Phys. Conf. Ser.*, vol. 2634, no. 1, p. 012034, Nov. 2023, doi: 10.1088/1742-6596/2634/1/012034.

[6] A. J. Ajwad and S. Tahmed Salim Rafid, "Enhancing Facial Image Clarity: Deblurring Gaussian blur with UNET++ Architecture," in *2023 26th International Conference on Computer and Information Technology*

DOI : https://doi.org/10.25139/inform.v10i2.9542

(ICCIT), IEEE, Dec. 2023, pp. 1–4. doi: 10.1109/ICCIT60459.2023.10441021.
[7] Q. Qi, J. Guo, C. Li, and L. Xiao, "Blind face images deblurring with enhancement," *Multimed. Tools Appl.*, vol. 80, no. 2, pp. 2975–2995, 2021, doi: 10.1007/s11042-020-09460-x.
[8] C. Cai, H. Meng, and Q. Zhu, "Blind deconvolution for image deblurring based on edge enhancement and noise suppression," *IEEE Access*, vol. 6, pp. 58710–58718, 2018, doi: 10.1109/ACCESS.2018.2874980.
[9] R. Yasarla, F. Perazzi, and V. M. Patel, "Deblurring Face Images Using Uncertainty Guided Multi-Stream Semantic Networks," *IEEE Trans. Image Process.*, vol. 29, pp. 6251–6263, 2020, doi: 10.1109/TIP.2020.2990354.
[10] Y. Pang, J. Mao, L. He, H. Lin, and Z. Qiang, "An Improved Face Image Restoration Method Based on Denoising Diffusion Probabilistic Models," *IEEE Access*, vol. 12, no. January, pp. 3581–3596, 2024, doi: 10.1109/ACCESS.2024.3349423.
[11] R. Wang, W. Li, R. Qin, and J. Z. Wu, "Blur image classification based on deep learning," *IST 2017 - IEEE Int. Conf. Imaging Syst. Tech. Proc.*, vol. 2018-Janua, pp. 1–6, 2017, doi: 10.1109/IST.2017.8261503.
[12] R. Wang, W. Li, and L. Zhang, "Blur image identification with ensemble convolution neural networks," *Signal Processing*, vol. 155, pp. 73–82, 2019, doi: 10.1016/j.sigpro.2018.09.027.
[13] S. Tiwari, "A blur classification approach using deep convolution neural network," *Int. J. Inf. Syst. Model. Des.*, vol. 11, no. 1, pp. 93–111, 2020, doi: 10.4018/IJISMD.2020010106.
[14] M. Tripathi, "Facial image denoising using AutoEncoder and UNET," *Herit. Sustain. Dev.*, vol. 3, no. 2, pp. 89–96, 2021, doi: 10.37868/hsd.v3i2.71.
[15] Z. Lian and H. Wang, "An image deblurring method using improved U-Net model based on multilayer fusion and attention mechanism," *Sci. Rep.*, vol. 13, no. 1, 2023, doi: 10.1038/s41598-023-47768-4.
[16] A. Tharwat, "Classification assessment methods," *Appl. Comput. Informatics*, vol. 17, no. 1, pp. 168–192, 2018, doi: 10.1016/j.aci.2018.08.003.
[17] A. Horé and D. Ziou, "Image quality metrics: PSNR vs. SSIM," *Proc. - Int. Conf. Pattern Recognit.*, no. March, pp. 2366–2369, 2010, doi: 10.1109/ICPR.2010.579.
[18] D. R. I. M. Setiadi, "PSNR vs SSIM: imperceptibility quality assessment for image steganography," *Multimed. Tools Appl.*, vol. 80, no. 6, pp. 8423–8444, 2021, doi: 10.1007/s11042-020-10035-z.
[19] P. Corke, W. Jachimczyk, and R. Pillat, "Images and Image Processing," *Springer Tracts Adv. Robot.*, vol. 147, pp. 435–491, 2023, doi: 10.1007/978-3-031-07262-8_11.
[20] F. A.-I. A. Putra, A. R. Jatmiko, D. M. Putri, and A. H. Al-Fath, "Vehicle Licence Number Plate Recognition Using Convolution Neural Network for Traffic Violators in Indonesia," *Inf. J. Ilm. Bid. Teknol. Inf. dan Komun.*, vol. 9, no. 2, pp. 181–186, 2024, doi: 10.25139/inform.v9i2.8449.
[21] L. Lisda, K. Kusrini, and D. Ariatmanto, "Classification of Pistachio Nut Using Convolutional Neural Network," *Inf. J. Ilm. Bid. Teknol. Inf. dan Komun.*, vol. 8, no. 1, pp. 71–77, 2023, doi: 10.25139/inform.v8i1.5685.
[22] X. P. Shi, S. Y. Lin, M. L. Yang, C. C. Huang, and J. C. Lee, "Image deblurring by multi-scale modified U-Net using dilated convolution," *Sci. Prog.*, vol. 107, no. 1, pp. 1–24, 2024, doi: 10.1177/00368504241231161.

DOI : https://doi.org/10.25139/inform.v10i2.9542